ISSN (Print) 1226-1750
ISSN (Online) 2233-6656
Journal of Magnetics 18(3), 230-234 (2013) http://dx.doi.org/10.4283/JMAG.2013.18.3.230

Effects of Solution Concentration on the Structural and Magnetic Properties of $Ni_{0.5}Zn_{0.5}Fe_2O_4$ Ferrite Nanoparticles Prepared by Sol-gel

B. S. Yoo, Y. G. Chae, Y. M. Kwon, D. H. Kim, B. W. Lee, and Chunli Liu*

Department of Physics, Hankuk University of Foreign Studies, YongIn, Gyeonggi 449-791, Korea

(Received 28 June 2013, Received in final form 1 August 2013, Accepted 2 August 2013)

The $Ni_{0.5}Zn_{0.5}Fe_2O_4$ nanoparticles about 30 nm were prepared using sol-gel method with metal nitrates dissolved in 2-methoxyathanol. The concentrations of the metal nitrates are adjusted from 0.1 to 0.75 M in order to study the influence on the structural and magnetic properties. The structure and morphology characterization revealed that the crystallinity was improved and the nanoparticle size was increased with the nutrition solution concentrations up to 0.5 M. Degraded crystallinity together with decreased nanoparticle size were observed for concentration of 0.75 M. The saturation magnetization at room temperature reached maximum at 0.5 M, which can be explained by considering the crystallinity and size effect.

Keywords : NiZn ferrite, nanoparticles, sol-gel, magnetization, concentration effect

1. Introduction

Spinel ferrites are magnetic oxides which possess the general formula MFe_2O_4, where M is a divalent cation. The ferrites are especially favored in high frequency applications due to their high temperature ferromagnetism, high resistivity, low eddy current, and low-loss dielectric properties [1]. Over the past few years there have been increasing interests for developing nanocrystalline ferrite materials because the nanosized ferrite particles are able to exhibit unusual magnetic properties, such as superparamagnetism, increased Curie temperature, metastable cation distribution, etc., which are not observed in the bulk materials. It is important to understand the connections between the properties of ferrite nanoparticles and their preparation routes and conditions, so that the desired properties can be effectively enhanced through appropriately designed preparation processes for targeted applications.

NiZn ferrite is the solid solution of zinc ferrite ($ZnFe_2O_4$) and nickel ferrite ($NiFe_2O_4$). $ZnFe_2O_4$ is a normal spinel, with the Zn^{2+} cations occupying the tetrahedral A-sites and the trivalent Fe^{3+} cations occupying the octahedral B-sites. $NiFe_2O_4$ is an inverse spinel in which the A sites are occupied by Fe^{3+} ions and the B-sites by Fe^{3+} and Ni^{2+} ions. Although the Zn^{2+} ion itself has no magnetic moments, it is well-known that by substituting the Ni ions with Zn ions, the magnetic moments of $NiFe_2O_4$ can be enhanced, and normally the highest magnetic moments can be achieved with Zn composition of about 40%. Recent applications such as multi-layer chip inductors and electromagnetic interference (EMI) suppressions renewed the research interests in NiZn ferrites [2, 3]. Ferrite nanoparticles can be prepared through several major chemical approaches including co-precipitation [4, 5], hydrothermal [6], and sol-gel [7, 8]. As compared to other processes, sol-gel has the advantages of simple procedures and the prepared nanoparticles usually have a high degree of crystallinity with a uniform microstructure and better magnetic behaviors [7]. The reaction parameters of the sol-gel process, for example, the type of precursors used, reaction temperature and pH value, etc., have been reported to have direct effects on the properties of fabricated ferrite nanoparticles [7-12]. In this work, we prepared NiZn ferrite nanoparticles through the sol-gel method by dissolving the corresponding metal nitrates in 2-methoxythanol. We adjusted the concentration of the precursor solutions and investigated its effects on the structural and magnetic properties of ferrite nanoparticles.

*Corresponding author: Tel: +82-31-330-4733
Fax: +82-31-330-4566, e-mail: chunliliu@hufs.ac.kr

2. Experimental details

The preparation of NiZn ferrite nanoparticles was carried out by sol-gel in 2-methoxyethanol. Nickel nitrate [$Ni(NO_3)_2 \cdot 6H_2O$], zinc nitrate [$Zn(NO_3)_2 \cdot 6H_2O$], and iron nitrate [$Fe(NO_3)_3 \cdot 9H_2O$] were first separately dissolved in 2-methoxyethanol in order to prepare solutions with molar concentration of 1 M. Then, the 3 metal nitrate solutions were mixed with molar ratio of Ni:Zn:Fe = 1:1:4 in 2-methoxyethanol. The volume of each solution used in the experiments was 2.5, 2.5, and 10 ml for Ni, Zn, and Fe nitrates, respectively. The total molar concentration of metals were adjusted to be 0.1, 0.3, 0.5, and 0.75 M by varying the volume of the 2-methoxyethanol in order to make the total solution to 150, 50, 30, and 20 ml. The mixed solution was stirred at room temperature for 3 hours, and then, heated at 90 ºC to evaporate all the liquids and to form a dried gel. To get rid of all organic gradients, the dried gel was heated at 100 ºC to burn in a self-propagating combustion manner as to form loose powder. Finally, the crystallization was performed at 600 ºC for 1 hour in an air ambient. Hereafter, we will identify the nanoparticles as S10, S30, S50, S75 for the concentration of precursor solution as 0.1, 0.3, 0.5, and 0.75 M.

The crystallinity of the obtained samples was characterized by x-ray diffraction (XRD). The surface morphology and microstructure of the nanoparticles were observed by using the scanning electron microscopy (SEM) and transmission electron microscopy (TEM), respectively. For TEM observations, the nanoparticles were first dispersed in acetone and one drop of the dispersed solution was put on the TEM grid. The magnetic properties of the nanoparticles were measured by Lakeshore 7400 vibrating sample magnetometer (VSM) in the range of 0-1 Tesla.

3. Results and Discussion

The XRD spectra from all 4 samples showed only peaks of the spinel crystal structures, indicating that the prepared nanoparticles are of single phase. Fig. 1(a) shows the XRD spectra of all samples. In the magnified view of the dominant diffraction [Fig. 1(b)], the (311) peak was observed at 35.38º for S10, S30, and S50, and it shifted to 35.40º for S75. The lattice constants were first calculated from peak position of (311) and (440) then took the average value, which turned out to be 8.405 Å for S10, S30, and S50, and 8.401 Å for S75. For comparison, we also prepared bulk $Ni_{0.5}Zn_{0.5}Fe_2O_4$ sample by conventional solid state reaction, and the lattice constant was measured to be 8.403 Å. Therefore, the lattice constant of the nanoparticles prepared with concentrations up to 0.5 M showed slightly enlarged lattice constant as compared to the bulk value, whereas the nanoparticles prepared with higher concentration of 0.75 M have lattice constants slightly smaller than the bulk value.

The XRD spectra also show a wider peak for S75, as shown in the inset of Fig. 1(b). The larger full width at half maximum (FWHM) may indicate a change in the crystallite size. The average crystallite sizes of the nanoparticles were estimated from the XRD spectra using the Scherrer equation [13] $D = 0.9\,\lambda/(\beta\cos\theta)$, where λ is the x-ray wave length (1.5406 Å) and β is the broadening of the peak at angle θ that can be estimated from the FWHM. For each sample, the dominated peak (311) was chosen for calculation. For nanoparticles prepared with concentrations from 0.1 to 0.5 M, the crystalline sizes increased from 30 to 34 nm, whereas those prepared with 0.75 M solutions showed much reduced size of ~24 nm. As compared to the nanoparticles, the NiZn ferrite prepared

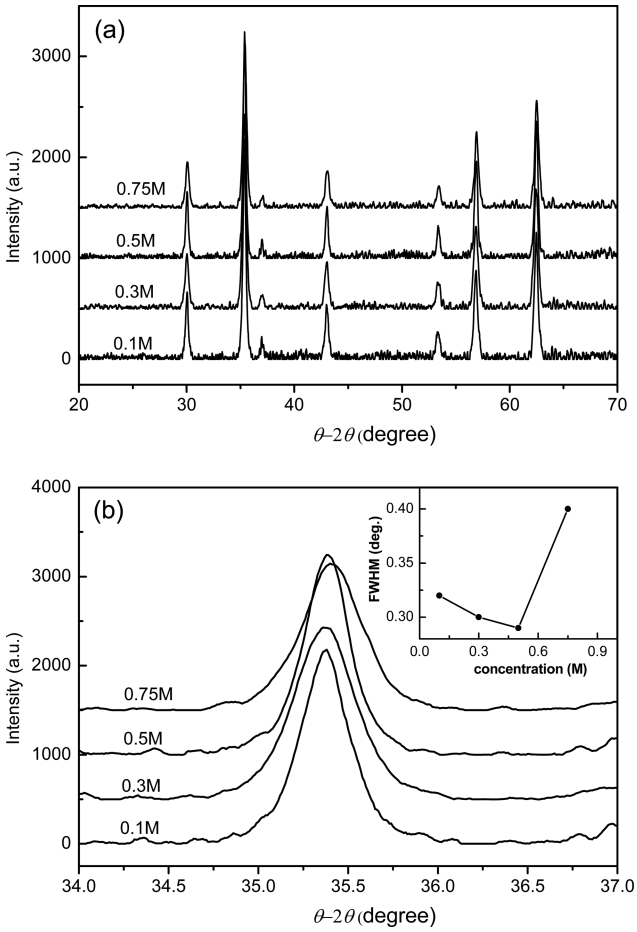

Fig. 1. XRD spectra from $Ni_{0.5}Zn_{0.5}Fe_2O_4$ nanoparticles prepared with different precursor concentrations. (a) 2θ range from 20 to 70º. (b) Magnified view of the (311) peak. The inset in (b) shows the change of FWHM vs. concentrations.

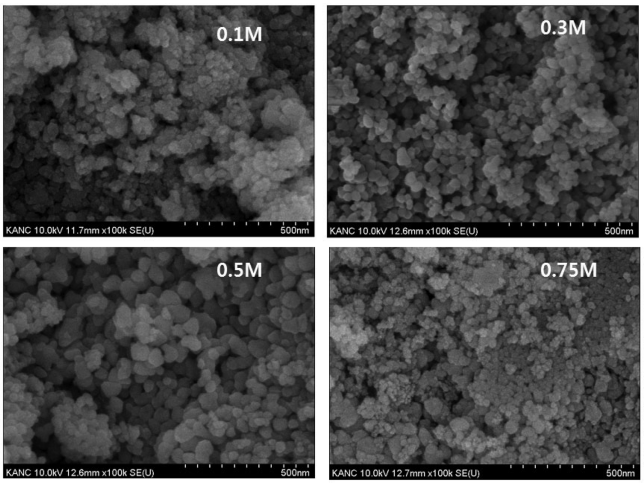

Fig. 2. SEM images from $Ni_{0.5}Zn_{0.5}Fe_2O_4$ nanoparticles, showing changes in the crystalline size with the precursor concentrations.

by solid-state reaction showed particle size of ~60 nm, which can be mostly contributed to the high temperature sintering process.

The SEM images in Fig. 2 show the typical morphology of the NiZn ferrite nanoparticles prepared with different precursor concentrations. Although the actual size of the nanoparticles is hard to tell from the SEM images due to the agglomeration, the trend is clear that the size of the nanoparticles increases with concentrations up to 0.5 M, and then decreases, which is consistent with the estimation from the XRD spectra.

TEM was employed to further investigate the microstructural properties of the NiZn ferrite nanoparticles as shown in Fig. 3(a)-(d). Nanoparticles are of sphere shape. The size distribution of nanoparticles plotted by measuring 40 particles in each sample is illustrated in Fig. 3(e). The change of crystalline size with the precursor concentration agrees well with the XRD and SEM observations. Fig. 3(f) showed the HR-TEM image of lattices in an S50 nanoparticle, and the fast Fourier transform pattern of the lattices is shown in Fig. 3(g). The high density points near the center form a cubic pattern, with the angle between |01| and |03| being 90°. The *d*-spacing calculated using point 1, 2, and 3 is 0.2972, 0.2101, and 0.2972 nm. Therefore, point 1 and 3 are most probably from the diffraction of (022) planes, whereas point 2 from the (004) plane of the spinel lattice [14]. The TEM image confirms that the nanoparticles are of cubic structure, and the lattice constant can be calculated to be 8.405 Å.

Field dependent magnetization of the NiZn ferrite nanoparticles were measured at room temperature. The magnetic properties were characterized by VSM in the field range of 0~1 Tesla. All samples showed clear hysteresis at room temperature. We observed from the magnetization-field (M-H) measurements that the saturation magnetization (Ms) increased with the concentration of the precursor solution up to 0.5 M, and then decreased for concentrations of 0.75 M. The M-H curves for the 4 samples are shown in Fig. 4, with their saturation magnetization showed in Fig. 4(b). The maximum value of Ms observed from S50 is close to those reported by

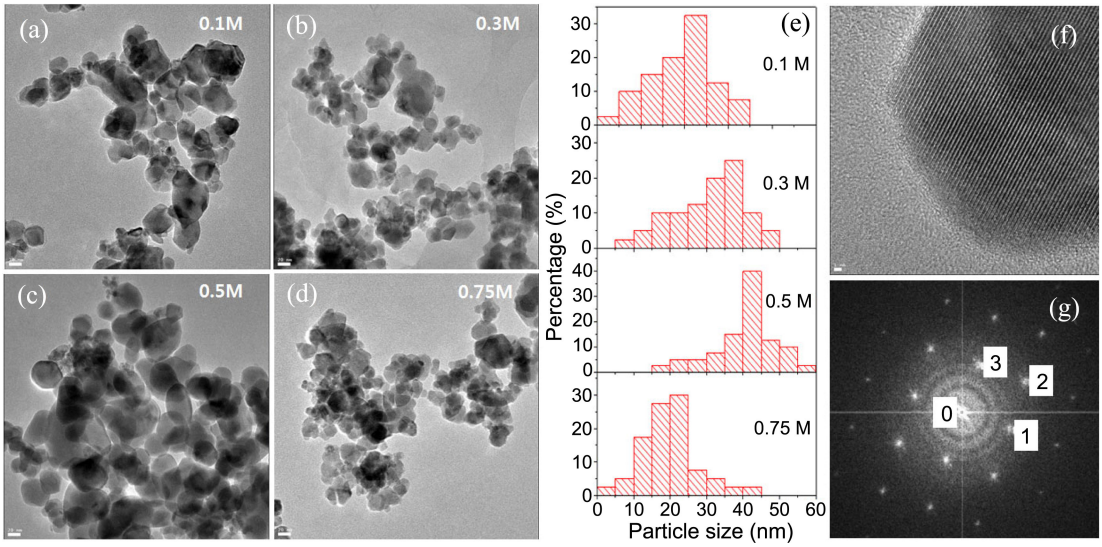

Fig. 3. (Color online) (a)-(d) TEM images from $Ni_{0.5}Zn_{0.5}Fe_2O_4$ nanoparticles prepared with different precursor concentrations. The scale bar in each image is for 20 nm. (e) The size distributions of nanoparticles prepared with different solution concentrations. (f) HR-TEM image of S50 showing the lattice of the nanoparticles. The scale bar is 1 nm. The Fast Fourier transform pattern obtained from the lattice is shown in (g).

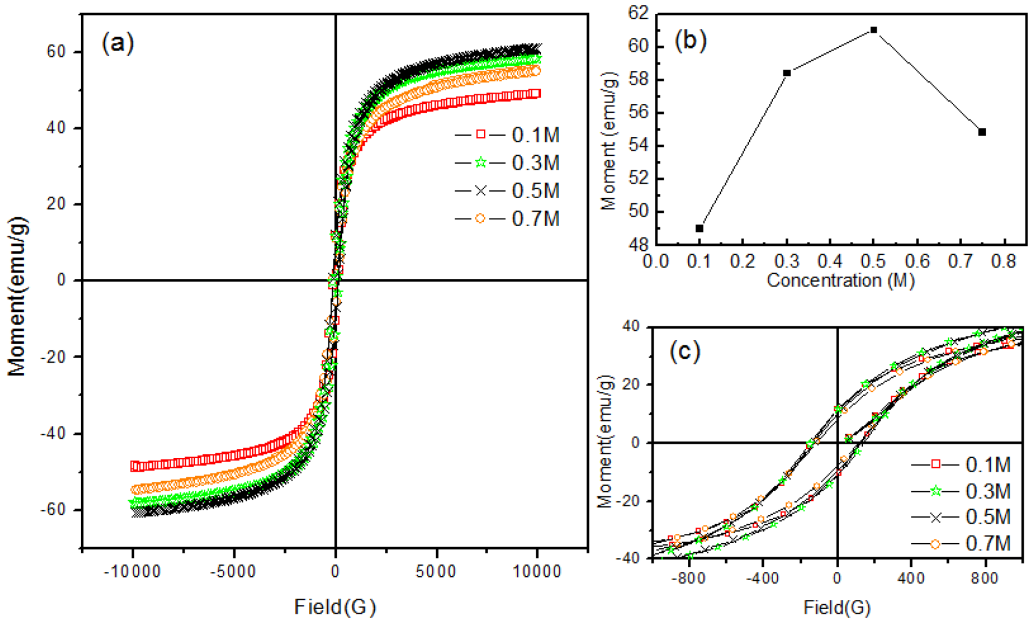

Fig. 4. (Color online) (a) M-H curves of NiZn ferrite nanoparticles measured at room temperature. (b) Changes of saturation magnetization with the solution concentration. (c) Enlarged hysteresis curves near zero fields to show the coercivity.

other groups [15, 16]. The hysteresis near zero fields are enlarged and showed in Fig. 4(c). Therefore, except the changes in the saturation magnetization, the precursor concentrations in the investigated range seemed to have no obvious effects on the coercivity.

The saturation and coercivity of ferrite nanoparticles can be affected by many factors, such as particle size, lattice constant, crystallinity, etc. In this study, since the change in Ms showed a similar trend with the nanoparticle size and crystallinity, it is reasonable to consider the relationship among these parameters together with the effects of solution concentration. For most chemical reactions, the reaction rate increases with the concentration due to the increased possibilities of collisions between the precursor molecules. Our results imply that 0.5 M is an optimized concentration for the preparation of NiZn ferrite nanoparticles when using 2-methaxythanol as a solvent. This concentration may provide an appropriate reaction rate to form nanoparticles with good crystallinity and allow enough time for grain growths to form larger-sized particles. For concentration of 0.75 M, the reaction rates may be too high to allow complete reaction and optimum bonding of the atoms, resulting in a degraded crystallinity and smaller particle sizes. Since the magnetization of the ferrite materials is mainly determined by the interactions between Fe^{3+} on the A sites and Fe^{3+} on the B sites, better crystallinity improves magnetization [12], which explains the increased saturation magnetization up to 0.5 M. On the other hand, smaller particles prepared with 0.75 M possess higher surface energy and surface tension, which could results in reduced magnetization [7]. The coercivity measures the resistance of a ferromagnetic material to becoming demagnetized, and usually, the nanoparticles show larger coercivity than the corresponding bulk materials, especially when the particle size is close to the single domain limit. We also observed that the coercivity of the bulk sample prepared by solid state reaction is about half of the nanoparticles (data not shown). The similar value of coercivities in all 4 samples in this study implies the comparable domain status of these nanoparticles despite of the difference in solution concentration.

4. Conclusions

In conclusion, we have investigated the effects of the solution concentration on the crystallographic and magnetic properties of Ni-Zn ferrite nanoparticles. The crystallinity improved and the sizes of the nanoparticles increased with the solution concentrations up to 0.5 M, presumably due to the gradually optimized reaction rate in the reaction solution. The saturation magnetization showed parallel changes with crystallinity of this range. When the solution concentration increased to 0.75 M, high reaction rates resulted in smaller sized nanoparticles with degraded crystallinity and saturation magnetizations.

References

[1] A. Goldman, Modern Ferrite Technology, Springer, New York (2009).
[2] L. Li, L. Peng, Y. Li, and X. Zhu, J. Magn. Magn. Mater. **324**, 60 (2012).
[3] Q. Li, Y. Wang, and C. Chang, J. Alloys. Compd. **505**, 523 (2010).
[4] Dinesh Varshney and Kavita Verma, Mater. Chem. Phys. **140**, 412 (2013).
[5] W.-C. Hsu, S. Chen, P. Kuo, C. Lie, and W. Tsai, Mater. Sci. Eng. B **111**, 142 (2004).
[6] A. Dias, R. L. Moreira, N. D. S. Mohallem, and A. C. Persiano, J. Magn. Magn. Mater. **172**, L9 (1997).
[7] B. Parvatheeswara Rao, G. S. Rao, A. M. Kumar, K. H. Rao, Y. L. Murthy, S. M. Hong, C.-O. Kim, and C. G. Kim, J. Appl. Phys. **101**, 123902 (2007).
[8] W. C. Kim, Y. S. Yi, and C. S. Kim, J. Magnetics **5**, 111 (2000).
[9] A. E. Virden and K. O'Grady, J. Magn. Magn. Mater. **290**, 868 (2005).
[10] S. S. Jadhav, S. E. Shirsath, B. G. Toksha, S. M. Patange, D. R. Shengule, and K. M. Jadhav, Physica B **405**, 2610 (2010).
[11] S. M. Masoudpanah, S. A. SeyyedEbrahimi, J. Magn. Magn. Mater. **323**, 2643 (2011).
[12] K. P. Chae, W. O. Choi, J.-G. Lee, B.-S. Kang, and S. H. Choi, J. Magnetics **18**, 21 (2013).
[13] B. D. Cullity, Elements of X-ray Diffraction, 2nd ed. Addison-Wesley, Reading (1978).
[14] B. Fultz and J. M. Howe, Transmission Electron Microscopy and diffractometry of Materials, 3rd ed. Springer, NewYork (2007).
[15] S. Verma, P. A. Joy, and S. Kurian, J. Alloys. Compd. **509**, 8999 (2011).
[16] T. J. Shinde, A. B. Gadkari, and P. N. Vasambekar, J. Magn. Magn. Mater. **333**, 152 (2013).